Biochemical Pharmacology, Vol. 52, pp. 157–166, 1996.



ISSN 0006-2952/96/$15.00 + 0.00
PII S0006-2952(96)00176-1

# Enhancement of Ricin Toxin A Chain Immunotoxin Activity: Synthesis, Ionophoretic Ability, and *In Vitro* Activity of Monensin Derivatives

*Franco Dosio,*‡ Antonia Franceschi,† Maurizio Ceruti,* Paola Brusa,* Luigi Cattel* and Marco Colombatti†*

*Istituto di Chimica Farmaceutica Applicata, c.so Raffaello 31, 10125 Torino, Italy, and †Istituto di Immunologia e Malattie Infettive, Ospedale Policlinico Borgo Roma, Verona, Italy

**ABSTRACT.** Site-selective toxin delivery was achieved by coupling monoclonal antibody to the A chain subunit of ricin (RTA-IT). The cell-killing potency of RTA-IT can be drastically increased *in vitro* by using ionophores such as monensin. To reduce the intrinsic toxicity of monensin and to enhance its *in vitro* and *in vivo* activity, we synthesized 7 derivatives characterized by different lipophilicities. These derivatives were also analyzed for ionophoretic activity on intact cells, toxicity, and RTA-IT-enhancing activity. Two different RTA-IT were assayed on a human leukemia cell line. A correlation between lipophilicity, ionophoretic activity, and RTA-IT enhancement was observed. The compounds with the highest polar charge showed low intrinsic toxicity, revealed moderate ionophoretic activity, and were able to enhance RTA-IT only at high concentrations, whereas more lipophilic compounds (with a C28 tail or a phenyl group) showed significant ionophoretic activity and good enhancing properties. BIOCHEM PHARMACOL 52;1:157–166, 1996.

**KEY WORDS.** immunotoxin; monensin; ricin A chain; enhancer; drug targeting

Tumor-selective cytotoxic conjugates are produced by chemically cross-linking bacterial toxins (e.g., diphtheria toxin, *Pseudomonas* exotoxin A) or plant toxins (e.g., ricin, abrin) to vehicle molecules (e.g., antibodies, ligands) that bind target antigens or receptors at the cell surface. The potential of MAb-ligand-toxin conjugates (IT) for tumor immunotherapy has been established in experimental models, as well as in clinical trials [1].

Ricin is a toxic plant glycoprotein formed by two subunits linked by a disulphide bond: the A chain, RTA§, which catalytically inactivates the protein synthesis of the target cell; and the B chain (RTB), which binds nonselectively to cell surface carbohydrate structures and helps RTA translocation to the cytosol of the target cell [1].

IT made with monoclonal antibody (MAb) linked to RTA have been extensively studied *in vitro* and in animal models [2–7], and their antitumor potential clinically investigated [8–13]. Although RTA-IT show high target-cell selectivity and low *in vivo* toxicity [8, 9, 11–13], their antitumor potency is variable, depending on the internalization rate, intracellular distribution, target-cell type, and other parameters [14–22]. As a result, the clinical trials conducted with RTA-IT have met with limited success. The cell-killing potency of RTA-IT, however, can be drastically increased *in vitro* by using lysosomotropic amines (e.g., ammonium chloride, chloroquine), ionophores (e.g., monensin, nigericin), calcium antagonists (perhexiline, verapamil) or lysosomal enzyme inhibitors (e.g., leupeptin, pepstatin) in combination [14–22].

Monensin (**1**, Scheme 1), a well-characterized metabolite of *Streptomyces cinnamonensis*, is a monovalent carboxylic polyether ionophore able to regulate $Na^+/H^+$ exchange across the cell membrane [23, 24].

Monensin potentiates the cytotoxic effect of IT directed against different cell surface structures and entering the cell *via* different pathways [25, 26]. Several other properties make monensin a potential candidate for the enhancement of RTA-IT *in vivo:* a) it potentiates RTA-IT at nanomolar concentrations in cell lines of different histotypes [25, 26]; b) it can be delivered *in vivo* encapsulated in liposomes or cross-linked to carrier proteins (e.g., HSA) to decrease its clearance rate *in vivo* [3, 27]; and c) large amounts of monensin can be tolerated *in vivo* in animals following i.v. or i.p. inoculation [2, 3, 27, 28]. However, attempts at monensin and HSA-linked monensin application *in vivo* have highlighted several obstacles hampering its use in the clinic as a potentiator of RTA-IT. Among these: 1. fast clearance of unconjugated monensin; 2. blockage of its enhancing effect by serum factors [29, 30]; and 3. higher toxicity when injected intrathecally [2]. New monensin-derived mol-

‡ Corresponding author. Tel. ++39.11.6707697; FAX ++39.11.6707695; E-mail dosio@ch.unito.it.

§ *Abbreviations:* RTA, ricin A chain; IT, immunotoxin; Tfn, transferrin; HSA, human serum albumin; FITC, fluorescein isothiocianate; DCCD, dicyclohexylcarbodiimide.

Received 2 November 1995; accepted 1 March 1996.

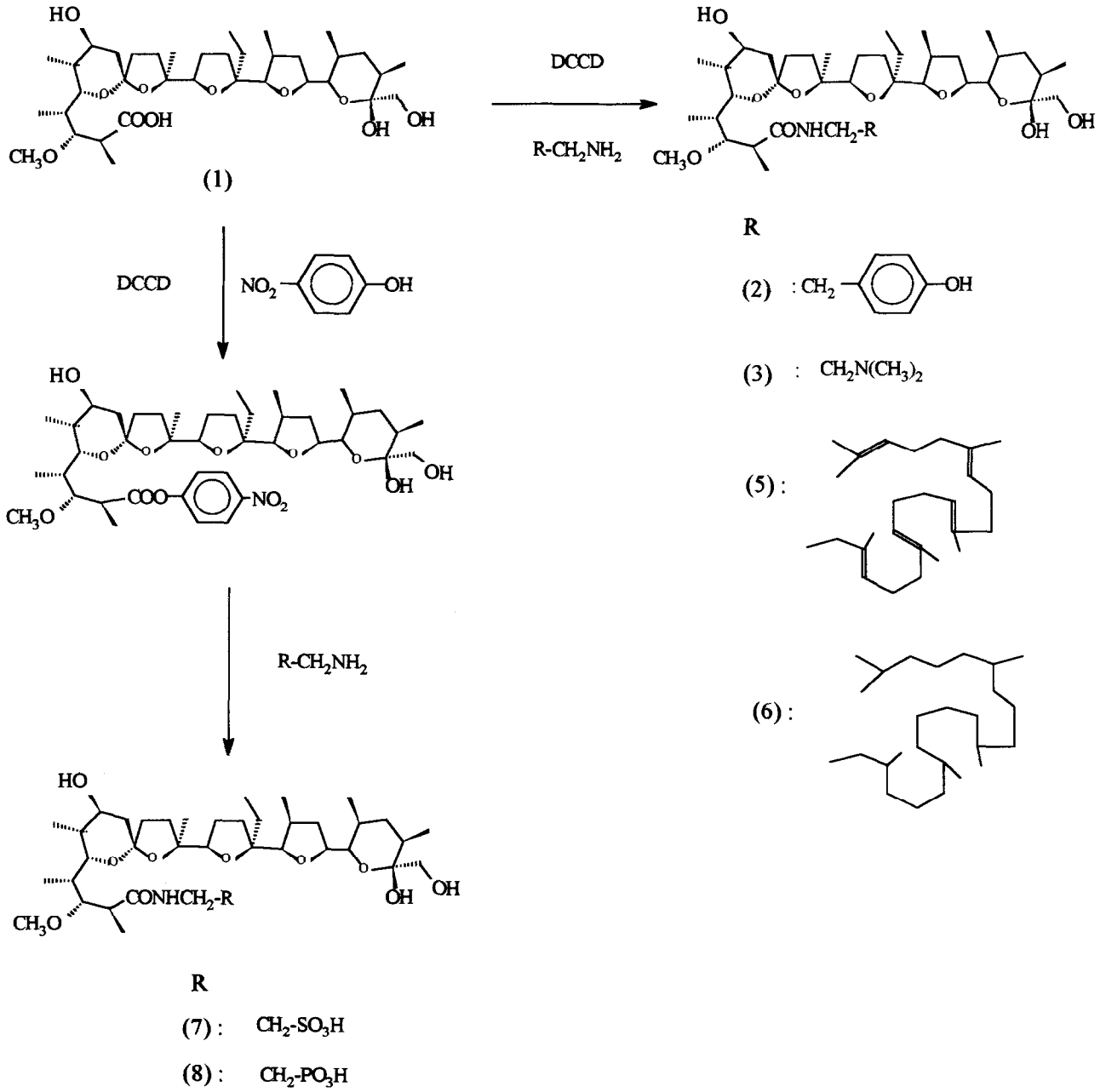


**Scheme 1. Synthetic route to monensin amide derivatives. Monensin acid was condensed with primary amino compounds in the presence of DCCD to provide monensyl tyramide (2), dimethylaminomethyl amide (3), squalene amide (5), and squalane amide (6). Alternatively, to provide monensyl taurinamide (7) or ciliatinamide (8), monensin acid was first condensed with 4-nitro-phenol in the presence of DCCD, and the 4-nitro-phenolate derivative then reacted with the amino compounds.**

ecules with properties apt to overcome some of the present limitations are, therefore, needed.

Treatment of cells with monensin leads to endosome and Golgi vacuolization [28, 31] which, in turn, affects the recycling of internalized molecules [32]. The molecular mechanisms by which monensin potentiates RTA-IT and accelerates their cell entry from intracellular compartments [33] have yet to be elucidated. Several hypotheses have been put forward to explain these aspects: 1. monensin may interact with intracellular membranes, facilitating the translocation of toxin molecules across the lipid bilayer; and 2. the ionophoretic properties of monensin may be required for toxin passage to the cytosol.

To tackle some of the questions related to the hypotheses mentioned above, we set out to study the ability of monensin analogues of increasing lipophilicity to enhance the cell-selective cytotoxicity of IT directed against two cell surface structures expressed by human leukemia cells, the transferrin receptor (TfnR) and the CD5 antigen. Modulation of lipophilicity was achieved by condensing the car-

boxyl group of monensin with several amines. For comparison, derivatives with higher polarity and, thus, increased solubility in water, were also prepared. The availability of a set of monensin derivatives also allowed us to approach some aspects pertaining to the structure-function relationship of monensin molecules.

## MATERIALS AND METHODS

### *Chemicals*

All chemicals were of reagent grade and were obtained from either Aldrich Chimica or Bracco-Merck (Milan, Italy). Monensin was purchased from Fluka Chemical Co. (Milan, Italy). $^1$H NMR spectra were recorded on a Jeol EX-400. Mass spectra were obtained on a VG Analytical 7070 EQ-HF spectrometer. IR were recorded on a Perkin-Elmer 781. Microanalyses performed on an elemental analyser 1106 (Carlo Erba Strumentazione) were within ± 0.4% of theoretical values.

### *Squalene Amine: (4E,8E,12E,16E)-4,8,13,17,21-pentamethyl-4,8,12,16,20-docosapentaenylamine*

$NH_3$ (ca. 5 mL) was liquefied at −80°C and anhydrous methanol (10 mL) previously cooled at −50°C was, then, added with continuous stirring. A solution of HCl in anhydrous methanol was added in drops up to pH 6.0; during this addition, a white precipitate formed. $NaBH_3CN$ (314 mg, 5 mmol) was then added, followed by 1,1′,2-tris-norsqualene aldehyde (1.92 g, 5 mmol). The reaction mixture was allowed to reach −25°C and left 12 hr at this temperature. It was, then, extracted with diethyl ether (100 mL) after addition of water (100 mL), dried over anhydrous sodium sulphate, and evaporated to dryness under vacuum. The resulting oil was purified by flash chromatography using diethyl ether/light petroleum 70:30, then diethyl ether and, finally, diethyl ether/methanol 95:5, to give squalene amine (482 mg, 25% yield). Anal. C, H, N. IR ($CHCl_3$) $\upsilon_{max}$ 2970, 2920, 2870, 1450, 1380 cm$^{-1}$. $^1$H-NMR ($CDCl_3$) δ: 1.55–1.64 (m, 20 H, allylic $CH_3$ and $CH_2CH_2N$), 1.96–2.05 (m, 18 H, allylic $CH_2$), 2.66 (m, 2H, $CH_2N$), 5.02–5.21 (m, 5H, vinylic CH). HRMS: found $M^+$, 385.3698. $C_{27}H_{47}N$ requires M, 385.3708; C, H, N.

### *Squalane Amine: 4,8,13,17,21-pentamethyldocosylamine*

Pd/C (10% Pd; 15 mg) was added to absolute ethanol (100 mL) under stirring, and the suspension was, then, put under $H_2$ atmosphere. Squalene amine (250 mg, 0.65 mmol) was added and left for 24 hr under $H_2$ atmosphere under stirring. The suspension was filtered to remove the catalyst and concentrated under vacuum. The crude product was purified by flash chromatography with diethyl ether and then diethyl ether/methanol 95:5 to remove impurities and, finally, with methanol to give 236 mg (92% yield) as a colorless viscous oil. Anal, C, H, N. IR ($CHCl_3$) $\upsilon_{max}$ 2960, 2920, 2860, 1460, 1380 cm$^{-1}$. $^1$H-NMR ($CDCl_3$) δ: 0.79–0.86 (m, 20 H, $CH_3$ and $CH_2CH_2N$), 0.98–1.40 (m, 33 H, alkylic $CH_2$ and CH), 2.59 (broad t, 2H, $CH_2N$). HRMS: found $M^+$, 395.4494. $C_{27}H_{57}N$ requires M, 395.4491; C, H, N.

### *Monensin Acid* (1)

Sodium monensin was dissolved in hot methanol and the solution filtered. Monensin was, then, precipitated by adding water to the cooled methanolic solution. This purification step was repeated twice. The white salt obtained was dried under vacuum (yield 83–87%). It was, then, dissolved in distilled chloroform and stirred vigorously for 1 hr at room temperature with a layer of aqueous perchloric acid (1 M) to convert the sodium salt into the acid form of monensin. The chloroform layer was washed with distilled water until the washings were neutral, and then evaporated to dryness. The obtained crystals were dried under vacuum and stored at −20°C.

To synthesize the reactive intermediate monensin 4-nitrophenolate, 500 mg of monensin acid (0.745 mmol) were dissolved in 10 mL of freshly prepared dry tetrahydrofuran (THF) and maintained at 5°C. 4-nitrophenol (160 mg, 1.15 mmol) and DCCD (250 mg, 1.2 mmol), dissolved in 3 mL of THF, were added and the reaction was maintained at 5°C for 24 hr. The precipitated dicyclohexylurea was removed by centrifugation and the reaction mixture purified by flash chromatography (2 × 20 cm $SiO_2$ Merck) using ethyl acetate/methylene chloride 15:85 and, then, 30:70. The fractions containing monensin 4-nitrophenolate were collected and dried under vacuum to obtain 450 mg of white crystalline product. Yield 76%. Rf = 0.38 in EtOAc-$CH_2Cl_2$ (30:70). IR (KBr) $\upsilon_{max}$ cm$^{-1}$: 1765, 1525, 1350, 2950. $^1$H-NMR (400 MHz, $CDCl_3$) δ: 8.27 (d, J = 9.06 Hz, H arom), 7.37 (d, J = 9.06 Hz, H arom), 4.48 (d, J = 8.8 Hz OH 2nd), 4.38 (br, OH 3rd), 4.31 (dt, J = 3.1, 8.1, 20H), 4.11 (dd, J = 2.2, 9.5, 5H), 3.94 (d, J = 4.4, 17H), 3.85 (m, 21H), 3.83 (br, 7H), 3.76 (t, J = 4.9 3H), 3.56 (dd, J = 5.5, 9.2, 13H), 3.45 (br, 26H), 3.39 (s, 35H), 2.98 (dq, J = 4.2, 6.9, 2H), 2.65 (br, OH 1st), 0.85–2.30 pattern of 45 protons. FAB-MS m/z: 814.4354 $(M + Na)^+$, Calcd for $C_{42}H_{65}NaNO_{13}$: 814.4356; C, H, N, O.

### *Monensin Methyl Ester* (4)

To synthesize this compound, the procedure described by Tohda *et al.* [34] was followed using methyl iodide and 1,8-diazabicyclo[5.4.0]undecene (Scheme 2).

The tyramide **(2)**, N,N-dimethylaminoethylamide **(3)**, squalene amide **(5)**, and squalane amide **(6)** derivatives of monensin were prepared using essentially the same procedure as in Scheme 1: Monensin acid (200 mg, 0.3 mmol) was stirred at 5°C for 30 min in 2 mL of dry dimethylformamide (DMF) or THF and, then, DCCD (64 mg, 0.31 mmol) was added. After being stirred for 1 hr, the reaction

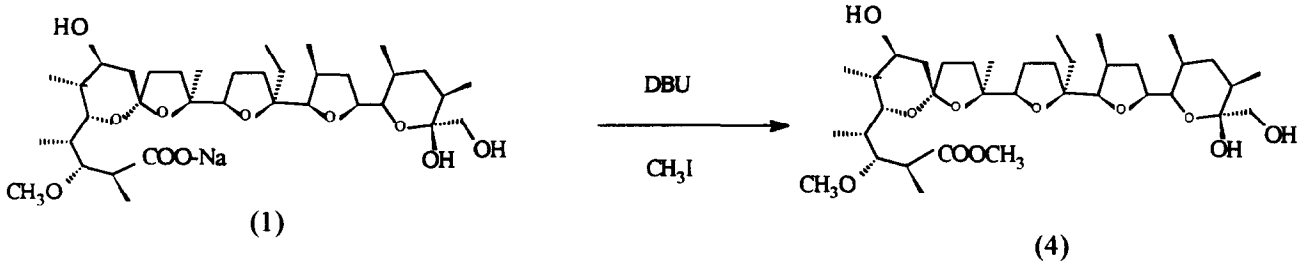


**Scheme 2. Synthetic route to monensin methylester derivative (4). Monensin sodium salt was reacted with methyl iodide and 1,8-diazabicyclo[5.4.0]undecene.**

was treated with 0.4 mmol of the corresponding amine: tyramine, N,N-dimethylethylenediamine, squalene, and squalane amine dissolved in 1 mL of dry DMF. Stirring was continued at 5°C for 24 hr. The mixture was evaporated under vacuum and the residue suspended in ethyl acetate and filtered off. To remove all the precipitated dicyclohexylurea, this step was repeated 3 times. The crude product was purified by flash chromatography on 230–400 mesh silica gel.

### *Monensin Tyramide* (2)

Elution mixture: methylene chloride/ethyl acetate 85:15 and, then, 5:95 to give 170 mg of pure **2.** Rf = 0.28 in $CH_2Cl_2$- MeOH (90:10). IR ($CHCl_3$) $\nu_{max}$ $cm^{-1}$: 1650 (C=O). $^1$H-NMR (400 MHz, $CDCl_3$) δ: 7.03 (d, J = 8.24 Hz, H arom), 6.79 (d, J = 8.40 Hz, H arom), 4.25 (dt, J = 3.1, 8.1, 20H), 4.11 (dd, J = 2.2, 9.5, 5H), 3.97 (d, J = 4.4, 17H), 3.85 (m, 21H), 3.65 (t, J = 4.9 3H), 3.56 (dd, J = 5.5, 9.2, 13H), 3.40 (br, 26H), 3.30 (s, 35H), 2.83 (dq, J = 4.0, 6.5, 2H), 2.65 (t, J = 5.2 Hz, CH-Ph), 0.85–2.30 pattern of 45 protons. FAB-MS m/z: 812.501 $(M + Na)^+$, Calcd for $C_{44}H_{71}NaNO_{11}$: 812.4925; C, H, N, O.

### *Monensin Dimethylaminoethylamide* (3)

Reaction solvent THF: Elution mixture ethyl acetate/methanol/ammonia 97.5:2:0.5 and, then, 96:3:1 to give 167 mg of pure **3.** Rf = 0.22 in EtOAc-MeOH -$NH_3$ (70:28:0.2). IR ($CHCl_3$) $\nu_{max}$ $cm^{-1}$: 1650. $^1$H-NMR (400 MHz, $CDCl_3$) δ: 4.41 (dt, J = 3.1, 8.1, 20H), 4.2 (dd, J = 2.2, 9.5, 5H), 4.01 (d, J = 3.4, 17H), 3.91 (br, 7H), 3.85 (m, 21H), 3.60 (dd, J = 5.5, 8.9, 13H), 3.42 (s, 35H), 3.38 (t, J = 7.5 Hz, CH-NCO), 2.90 (dq, J = 3.6, 7.0 Hz, 2H), 0.85–2.30 pattern of 45 protons. FAB-MS m/z: 763.498 $(M + Na)^+$, Calcd for $C_{40}H_{72}NaN_2O_{10}$: 763.508; C, H, N, O.

### *Monensin Squalene Amide* (5)

Elution mixture: methylene chloride/methanol 99:1 and, then, 96:4 to give 150 mg of pure **5.** Rf = 0.58 in $CH_2Cl_2$-MeOH (90:10). IR ($CHCl_3$) $\nu_{max}$ $cm^{-1}$: 1650. $^1$H-NMR (400 MHz, $CDCl_3$) δ: 5.1 (m, vinyl CH- Squalene), 4.41 (dt, J = 3.0, 8.3 Hz, 20H), 4.2 (dd, J = 2.0, 9.4 Hz, 5H), 3.85 (m, 21H), 3.42 (s, 35H), 2.95 (m, 2H), 0.85–2.30 pattern of 45 protons, 1.99 (m, methylene CH-Squalene), 1.6 (s, methyl CH-Squalene). FAB-MS m/z: 1060.9010 $(M + Na)^+$, Calcd for $C_{63}H_{107}NaNO_{10}$: 1060.7792; C, H, N, O.

### *Monensin Squalane Amide* (6)

Elution mixture: methylene chloride/methanol 99:1 and, then, 96:4 to give 110 mg of pure **6.** Rf = 0.68 in $CH_2Cl_2$-MeOH (90:10). IR ($CHCl_3$) $\nu_{max}$ $cm^{-1}$: 1650. $^1$H-NMR (400 MHz, $CDCl_3$) δ: 4.41 (dt, J = 3.0, 8.3 Hz, 20H), 4.2 (dd, J = 2.0, 9.4 Hz, 5H), 3.85 (m, 21H), 3.42 (s, 35H), 2.95 (m, 2H), 0.85–2.30 pattern of 45 protons, 1.25 (m, methylene CH-Squalane), 0.87 (m, methyl CH-Squalane). FAB-MS m/z: 1070.8110 $(M + Na)^+$, Calcd for $C_{63}H_{117}NaNO_{10}$: 1070.8575; C, H, N, O.

### *Monensin Taurine Amide* (7)

To a solution of 400 mg of monensin 4-nitrophenolate (0.5 mmol) in 5 mL of dry pyridine were added 160 mg of taurine (2-aminoethanesulfonic acid) (1.28 mmol), previously dissolved in 2.3 mL of distilled water. The solution was maintained vigorously stirred for 48 hr at room temperature. After evaporation under vacuum, the unreacted taurine was filtered off in ethyl acetate and the crude product purified by flash chromatography using methylene chloride/ethyl acetate 95:5 and, then, methylene chloride/ethyl acetate/methanol 55:30:15. The white powder was, then, crystallized from acetone/ethyl acetate to give 383 mg of pure **7.** M.p. 161–162°C. Rf = 0.0.8 in $CH_2Cl_2$-MEOH (90:10). IR (KBr) $\nu_{max}$ $cm^{-1}$: 1650 (C=O), 1255 ($SO_2$ asymm), 1050 ($SO_2$ sym). $^1$H-NMR (400 MHz, $d^6$-DMSO) δ: 4.35 (dt, J = 3.1, 7.8, 20H), 4.15 (dd, J = 2.5, 8.9, 5H), 3.95 (br, 7H), 3.83 (m, 21H), 3.35 (s, 35H), 3.11 (m, CH-taurin), 0.85–2.30 pattern of 45 protons. FAB-MS m/z: 823.397 $(M + 2Na)^+$, Calcd for $C_{38}H_{67}Na_2NO_{13}S$: 823.4128; C, H, N, O, S.

### *Monensin Ciliatine Amide* (8)

To a solution of 400 mg of monensin 4-nitrophenolate (0.5 mmol) in 10 mL of dry pyridine were added 160 mg of ciliatine (2-aminoethylphosphonic acid) (1.28 mmol) previously dissolved in 4.5 mL of distilled water. The solution was vigorously stirred for 5 days at room temperature. After

evaporation under vacuum, the unreacted ciliatin was filtered off in ethyl acetate and the crude product was purified by 5 preparative TLC plates (20 × 20 cm × 1 mm, Bracco-Merck, Milan, Italy), eluent methylene chloride/methanol 80:20 to give 85 mg of pure **8**. Rf = 0.18 in $CH_2Cl_2$-MeOH (80:20). IR ($CHCl_3$) $\nu_{max}$ $cm^{-1}$: 1650 (C=O), 1280 (PO). $^1$H-NMR (400 MHz, d$^6$-DMSO) δ: 4.28 (dt, J = 3.1, 7.8, 20H), 4.20 (dd, J = 2.5, 8.9, 5H), 4.05 (d, J = 3.4, 17H), 3.91 (br, 7H), 3.85 (m, 21H), 3.60 (dd, J = 5.5, 8.9, 13H), 0.85–2.30 pattern of 45 protons. $^{32}$P-NMR δ: 19.7, disacc. dt J = 17.09, 21.9 Hz. FAB-MS m/z: 823.412 (M + 2Na-H)$^+$, Calcd for $C_{38}H_{68}Na_2NO_{13}P$: 823.4228; C, H, N, O, P.

LIPOPHILICITY (RM) DETERMINATION. The lipophilic character of the synthesized compounds was determined by a chromatographic Rm method [35, 36]. Solutions of compounds were spotted 1 cm above the bottom of silanized silica gel TLC plates (20 × 20 cm, RP-2, Bracco-Merck). The plates were developed with various mixtures of water-methanol (from 50 to 90% in methanol). Then, the plates were dried and sprayed with a 4% solution of vanillin in methanol and 2.5% concentrated sulphuric acid. After a few minutes of 80°C, reddish spots appeared. The Rm were calculated from the following expression: Rm = log[(1/Rf)-1] where *Rf* is the distance travelled by the compound divided by the distance travelled by the solvent front (18 cm). The values reported in Fig. 1 represent the mean of 4 different chromatographic runs for each monensin derivative.

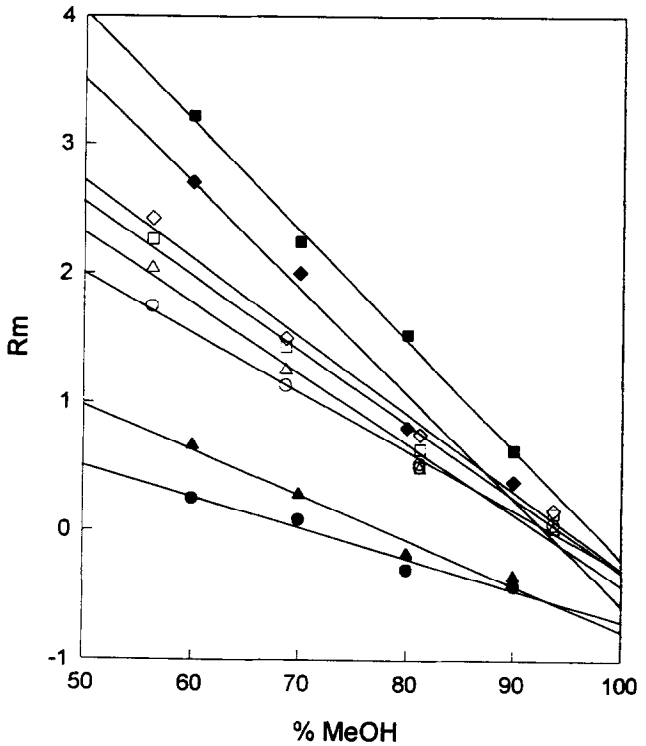


**FIG. 1. Linear relationship between Rm values and methanol concentration in the mobile phase. The values reported represent the mean of 4 values: 1 (○), 2 (◇), 3 (△), 4 (□), 5 (■), 6 (◆), 7 (●), 8 (▲).**

### *Biological*

CELLS. The Jurkat, a human T-lymphoblastoid cell line CD5+, was used. Jurkat cells were maintained by serial passage in RPMI 1640 (Seromed, Berlin, Germany) + 10% fetal calf serum (Seromed) and gentamicin at 37°C in 5% $CO_2$ in humidified atmosphere.

IMMUNOTOXINS. ST.1 (Fab')2-RTA (henceforth designated ST.1-RTA for brevity) IT to the CD5 differentiation antigen of human T lymphocytes was kindly supplied by Dr. P. Casellas (Sanofi Reserche, Montpellier, France). The preparation and properties of this IT have been described in detail previously [37]. Transferrin (Tfn)-RTA IT was synthesized and purified as described [38]. In all cytotoxicity assays, the concentration of IT is expressed as protein concentration.

PROTEIN SYNTHESIS ASSAYS. Protein synthesis measurements were performed to assay the intrinsic toxicity of monensin and its derivatives and to evaluate their RTA-IT enhancing activity.

a) Toxicity: protein synthesis was assayed by incubating 5 × $10^4$ Jurkat cells in 50 μL leucine-free RPMI, 5% fetal bovine serum in 96-well flat-bottomed microtitration plates (Costar, Cambridge, MA, U.S.A.). From a stock solution of 5 mM of monensin in DMSO, 10-fold dilutions were prepared. DMSO (1% final concentration) alone had no effect on cell culture. Monensin and its derivatives were, then, added to Jurkat cell microcultures and target cells incubated for 22 hr at 37°C in 5% $CO_2$ in a humidified atmosphere in 100 μL final volume. Final concentrations ranged from 500 μM to 0.5 nM. Under these conditions, in the absence of monensin or derivatives, the cells proliferate monoexponentially. One μCi of L-[U-$^{14}$C]-Leucine (316 mCi/mmole, DuPont, Boston, MA, U.S.A.) in 10 μL of RPMI was, then, added. After 2 hr, the cells were harvested onto glass fiber filters, washed with water, and dried. Radioactivity incorporated by the cells was, then, measured in a beta-spectrometer. The results are expressed as a percentage of the incorporation of control mock-treated cultures. The cytotoxicity of monensin or its derivatives was compared by taking the molar concentration required to inhibit 50% protein synthesis ($IC_{50}$).

b) Enhancement of RTA-IT cytotoxicity: Jurkat target cells (5 × $10^4$/well) were treated with various concentrations of different RTA-IT for 22 hr in the presence or in the absence of monensin or its derivatives, used at the highest nontoxic concentration. Protein synthesis was, then, measured as described above. Raw data expressed in cpm were also processed as above.

CYTOFLUOROMETRY. Tfn and anti-TfnR antibodies are internalized to low pH intracellular compartments [39]. We took advantage of the pH-dependent fluorescence of fluorescein isothiocianate (FITC)-labelled proteins [40] to investigate *in vivo* the ionophoretic activity of monensin and its derivatives.

Fluorescence emission of FITC-labelled molecules inter-

nalized to low pH compartments is decreased with respect to that of noninternalized surface-bound FITC-labelled molecules. Addition of monensin following internalization into acidic compartments leads to an increase of FITC emission due to monensin-driven neutralization of low pH intracellular organelles [41].

Tfn was labelled with FITC following described procedures [41]. An antiFITC mouse MAb (clone FL-D6) was from Sigma (St. Louis, MO, U.S.A.).

Jurkat cells ($3 \times 10^5$ in 50 μL RPMI 1640) were incubated for 1 hr at 4°C with a saturating amount of FITC-labelled Tfn. The cells were, then, washed twice with a cold solution of bovine serum albumin (BSA) 0.2% in phosphate saline buffer (0.1 M, pH 7), to remove unbound Tfn-FITC, and resuspended in 200 μL cold RPMI medium. The cells were, then, incubated at 37°C for 30 min to allow internalization of surface-bound molecules. The samples were, then, placed at 4°C and treated for 30 min with monensin or its derivatives at various concentrations (range 0.5–50 μM). AntiFITC MAb (1:100 final dilution) was also added to quench the fluorescent emission of non-internalized surface-bound FITC-labelled molecules. Under these conditions, only an intracellular fluorescent emission could be detected. In control mock-treated samples, monensin or its derivatives were omitted and only the diluent (DMSO) was added. Other control samples were treated as above, except that the temperature was kept at 4°C throughout washings and incubations. The fluorescence intensity expressed by the cells was, then, evaluated by running cell samples through an Epic-Profile II (Coulter, Hialeah, FL, U.S.A.) cytofluorometer with an exciting wavelength of 488 nm at 15 mW power. Fluorescence intensity values are expressed as mean fluorescence intensity (MFI). The difference in MFI between values obtained from samples treated with monensin or its derivatives and untreated samples (ΔMFI) was taken as a measure of their ionophoretic activity.

Experiments in Tables and Figs. are representative of 3–4 experiments; values represent the average of duplicate or triplicate samples (<10% standard error).

## RESULTS AND DISCUSSION

In an effort to obtain new RTA-IT enhancers with high activity and to investigate the possible correlation between the structure of monensin and its potentiating activity, seven structural analogues were synthesized (Schemes 1 and 2) and assayed: two compounds with an increased negative polarity (sulphate and phosphate group), and one with an ionizable positive charge (dimethylamino group). Three compounds with more lipophilic groups: a rigid phenyl group, and two long-chain structures of 28 carbon atoms: more rigid for the tris-nor squalene, more flexible for the tris-nor squalane. For comparison, we also prepared a methyl ester derivative of monensin to reduce the polarity of its carboxyl group.

Monensin **(1)**, obtained by treatment of commercially available sodium salt with perchloric acid, was condensed with several substituted primary amines in the presence of DCCD to provide monensylamide compounds **(3–6)** (Scheme 1). Due to the complete insolubility of taurine and ciliatine in organic solvents, a different synthetic approach involving the reactive 4-nitrophenolate ester was chosen to obtain more polar derivatives **(7, 8)** (Scheme 1).

### *Lipophilicity*

The partitioning of monensin and related derivatives between a stationary and polar mobile phase is a function of their structure. Thus, using the procedure described by G. L. Biagi *et al.* [35, 36] a relative lipophilicity factor, Rm, can be determined. Under these conditions, Rm values higher than that of monensin are suggestive of higher lipophilicity. From Fig. 1, it appears that only compounds **7** and **8** are more polar than monensin; all others are more lipophilic, in an increasing order, from **2** to **6.**

### *Toxicity*

The cytotoxicity of monensin and its derivatives was tested on the human T-lymphoblastoid Jurkat cell line (Table 1). Considering the $IC_{50}$ values, only compounds **7** and **8,** endowed with a highly negative charge, show a considerable reduction in toxicity, being 114–207-fold less toxic than the parent drug. Derivatives **2, 3,** and **4** are also less toxic (4–7-fold reduction in toxicity), whereas the more lipophilic squalene and, in particular, squalane derivatives were as toxic as monensin. Thus, the relatively higher toxicity of the derivatives correlates with a higher lipophilicity (Fig. 1 and Table 1) and the relatively higher toxicity of more apolar compounds might, thus, be a result of a facilitated interaction with the cell membranes. The reduced toxicity of the synthesized compounds with respect to the parent drug allowed us to test higher concentrations of monensin derivatives in RTA-IT potentiation assays.

### *Enhancement of RTA-Immunotoxins by Monensin and its Derivatives*

To evaluate the ability of monensin derivatives to enhance RTA-ITs, several concentrations of the various drugs and

**TABLE 1. Toxicity of monensin derivatives on Jurkat cell line***

| Compound | $IC_{50}$ (μM) |
|---|---|
| 1 | 1.4 ± 0.1 |
| 2 | 7.5 ± 0.5 |
| 3 | 5.3 ± 0.2 |
| 4 | 10 ± 1.1 |
| 5 | 4.6 ± 0.6 |
| 6 | 1.5 ± 0.5 |
| 7 | 290 ± 3.1 |
| 8 | 160 ± 4.2 |

* Jurkat cells were incubated with different concentrations of monensin or its derivatives for 22 hr. Protein synthesis inhibition was, then, measured, based on L-[U-$^{14}$C]-Leucine incorporation, and $IC_{50}$ values were determined.

different concentrations of IT were added to Jurkat cell microcultures.

Two different ITs directed against different antigens expressed by the Jurkat cells were tested: one composed of a monoclonal antibody ST.1 (antiCD5) conjugated with RTA, and the other of human transferrin linked to RTA. The antiCD5 RTA-IT was chosen for our study because of its relevance in the treatment of human diseases. In fact, antiCD5 IT have been used *ex vivo* for bone marrow purging, and CD5 IT-based therapy has also been extensively investigated clinically in a broad spectrum of pathologies [42, 43]. Similarly, Tfn IT has been proposed for the treatment of solid tumors of various histotypes, particularly those affecting the central nervous system (CNS) [42, 43]. Furthermore, inasmuch as Tfn is not species-specific [27], it allows the use of a large panel of target human, rat, and mouse cell lines for comparisons.

The optimal dose of 1 to be used in *in vitro* experiments is 50 nM, as reported in previous publications [2, 27]. At higher doses of **1**, no increase in RTA-IT enhancement was observed, and a monensin-dependent toxicity began to appear (not shown). Figure 2 shows the potentiation of the cytotoxic activity of ST.1-RTA and of free RTA by **1**. As shown in Fig. 2, the cell-selective cytotoxicity mediated by ST.1-RTA was increased 1140-fold, whereas the noncell-selective toxicity of unconjugated RTA was increased only 10-fold. These data can be compared to the cytotoxicity of native ricin. These results suggest that both cell surface binding and, as reported by Griffin *et al.* [44], the presence of a reducible disulphide bond between RTA and the carrier molecule are necessary for monensin effect. Due to the different toxicity shown by the various derivatives, several concentrations were assayed in each case in an RTA-IT dose-response assay.

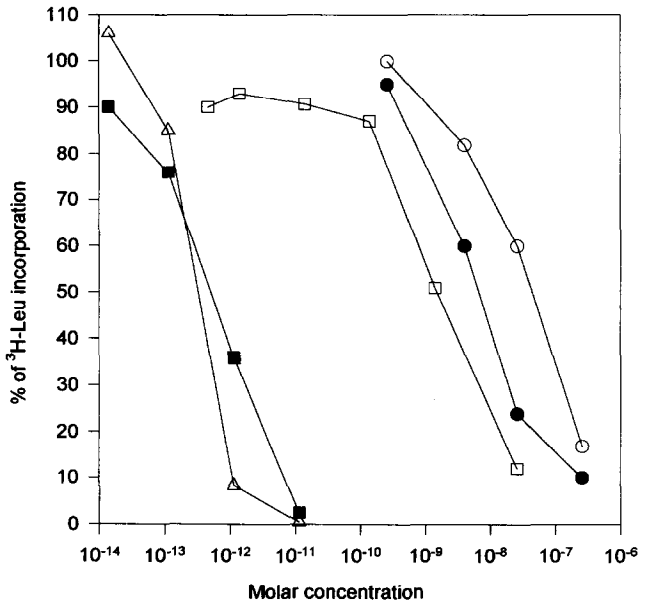


**FIG. 2. Enhancement of ST.1-RTA and RTA cytotoxicity by monensin. Jurkat cells were incubated for 22 hr with either ST.1-RTA IT (squares) or ricin A chain (circle) in the absence (open symbols) or in the presence (filled symbols) of 50 nM monensin. Protein synthesis was, then, measured. For comparison, cytotoxicity of native ricin is presented (triangle).**

The cytotoxicity of the two IT in the absence of potentiators is reported in Table 2: ST.1-RTA showed low cytotoxicity ($IC_{50}$ = 1140 pM), whereas Tfn-based IT was 50-fold more active ($IC_{50}$ = 26 pM). This allowed us to correlate the activity of the enhancers on a rapid internalization, rapid recycling model (Tfn) in comparison with a slower one (antiCD5).

Overall, the data reported in Table 2 illustrate uniform patterns as regards the RTA-IT enhancing activity of monensin and its derivatives: in general, the extent of RTA-IT potentiation depends on the type of immunotoxin used for all drugs (monensin included) and reflects the cytotoxic activity of RTA-IT observed in the absence of enhancers.

In particular: 1) Compounds **2**, **5**, and **6** showed an RTA-IT potentiating activity comparable to **1**. Compound **6** showed a significatively higher (2-fold) potentiating activity in comparison with the parent drug. However, it must be noted that the RTA-IT enhancement observed with compounds **2**, **5**, and **6** was achieved at a 10-fold higher concentration than **1**, whereas the most polar compounds **7** and **8** required a 1000-fold higher concentration. A higher concentration could be used in this case due to their lower intrinsic toxicity. As previously described, **1** cannot be tested at concentrations higher than 50 nM, due to its high intrinsic toxicity.

2) Derivatives with a positive ionizable charge (e.g., compound **3**) or with a reduced negative charge (e.g., compound **4**) showed no RTA-IT enhancing activity at the concentrations tested.

The mechanism of potentiation of toxin conjugates by monensin has not yet been fully elucidated. Monensin affects cells in many ways, apparently as a consequence of profound changes in the cytoplasmic $Na^+/K^+$ balance [31].

When RTA-IT are directed against target cells, the most important consequence of the presence of monensin is that the conjugate tends to accumulate in endocytic vacuoles, which appear as enlarged vesicles and in a finely structured tubovesicle system, whereas entry and accumulation of the RTA-IT into the lysosomes is considerably reduced [45]. These phenomena are probably essential to prevent RTA degradation and allow maximal cytotoxic efficacy.

Coated vesicles and endosomal vacuoles are known to be the site of dissociation of Tfn from its receptor [39]. Therefore, analogous to Tfn, a surface-endosome-surface routing can be suggested for Tfn-RTA. In the case of antiCD5 RTA-IT, however, it has been shown that the cell intoxication process involves a surface-Golgi-surface recycling route [14]. The different intracellular routing of the two RTA-IT used in our experiments may account for the greater cytotoxicity of Tfn-RTA in the absence of potentiators. On the other hand, inasmuch as monensin functions intracellularly by altering the Golgi, it could be spec-

**TABLE 2. Comparative RTA immunotoxin enhancement of Jurkat cell line by monensin and derivatives***

| Immunotoxin | $IC_{50}$ (pM)/Fold-Potentiation | | | |
|---|---|---|---|---|
| (Enhancer concentration (μM) | 0.05 | 0.5 | 5 | 50 |
| ST.1-RTA (1140 pM)† | | | | |
| +1 | 0.46/2478 | | | |
| +2 | 2.8/407 | 0.44/2590 | | |
| +3 | 840/1.3 | 800/1.0 | | |
| +4 | 1100/1.0 | 810/1.4 | | |
| +5 | 240/5.0 | 0.4/2590 | | |
| +6 | 1.7/670 | 0.28/4071 | | |
| +7 | 810/1.0 | 710/1.0 | 500/2.1 | 1.8/633 |
| +8 | 1100/1.0 | 750/1.5 | 0.9/1267 | 0.29/3930 |
| Tfn-RTA (26 pM)† | | | | |
| +1 | 0.18/144 | | | |
| +2 | 26/1.0 | 0.16/162 | | |
| +3 | 26/1.0 | 26/1.0 | | |
| +4 | 26/1.0 | 26/1.0 | 26/1.0 | |
| +5 | 15/1.7 | 0.17/153 | | |
| +6 | 26/1.0 | 0.1/260 | | |
| +7 | 26/1.0 | 26/1.0 | 0.4/65 | 0.2/130 |
| +8 | 15/1.7 | 15/1.7 | 13/1.8 | 0.24/108 |

* Cytotoxicity assay on Jurkat cells was induced by incubation with different concentrations of RTA-ITs and drugs for 22 hr. Protein synthesis inhibition was then measured based on L-[U-$^{14}$C]-Leucine incorporation and $IC_{50}$ values were determined. †$IC_{50}$ values of IT without addition of enhancers.

ulated that the greater potentiation observed with anti-CD5-RTA is due to the preferential delivery of ST.1 immunotoxin to the Golgi or to the Golgi-related compartments. However, it must be noted that, at the low concentrations used in our assays, monensin seems unable to alter the pH of intracellular compartments [29].

### *Ionophoretic Activity*

The cytofluorometric assays employed by us rendered possible the evaluation of the ionophoretic activity of monensin and its derivatives in intact cells. In fact, the difference in MFI between treated samples vs control samples (i.e., ΔMFI) is due to their ability to neutralize the low pH of intracellular compartments. It must be mentioned, however, that the ionophoretic activity of the various compounds could be detected with a cytofluorometric assay only at concentrations higher than those required to achieve RTA-IT enhancement in protein synthesis inhibition assays. The cytofluorometric assay was carried out with Tfn-FITC because Tfn is directed to low pH prelysosomal compartments [46] and its internalization cycle proceeds with fast kinetics [39]. As illustrated in Fig. 3, monensin showed the highest pH neutralizing effect, plateauing at 20–50 μM. Among the derivatives, those endowed with higher lipophilic properties (i.e., **5** and **6**) and **2** displayed a relatively higher ionophoretic activity (ΔMFI > 1), whereas the negatively charged **7** and **8** analogues, as well as **4**, showed a lower ionophoretic activity (ΔMFI < 1). Thus, a correlation was found between ionophoretic activity and lipophilic properties of the various compounds assayed. Lipophilicity is known to play an important role in penetration of various compounds into the cell membranes; in particular, lipophilic derivatives of ionophores allowed a more rapid transport of metal ions [47]. In our case, we can correlate the Rm values and the ionophoretic activity expressed as ΔMFI. It is likely that compounds **5** and **6** (approximately 3 times more lipophilic than monensin) and **2** (characterized by a rigid phenyl group) are able to increase ion traffic and, therefore, display relatively greater ionophoretic properties in the cytofluorometric assay. It must be noticed, however, that, in our assay, monensin displayed the greatest ionophoretic activity and, therefore, its lipophilicity/size ratio may be the most advantageous in performing a rapid ion transport, as evidenced by cytofluorometry.

Furthermore, a direct correlation between cell toxicity and ionophoretic activity can be appreciated in Fig. 3 and Table 1. In particular, the low ΔMFI shown by compounds **7** and **8** parallels the strong reduction in toxicity observed with monensin. This may be due to a reduced solubility in the cell membranes and/or to less efficient $Na^+$ ion transport by these compounds.

How ionophoretic activity and lipophilicity relate to the ability to potentiate RTA-IT is still under investigation.

As shown in Fig. 3 and Table 2, we found that a correlation also exists between the ionophoretic properties of the various compounds and their RTA-IT potentiating effect. Cell intoxication by RTA is facilitated by neutral or slightly alkaline pH [48]. It is, therefore, likely that compounds showing higher ionophoretic activity and, thus, greater pH neutralizing properties also display greater RTA-IT enhancing activities.

In conclusion, we show here that various structural analogues of the RTA-IT enhancer monensin may be less toxic than the parent drug, but also display variable enhancing

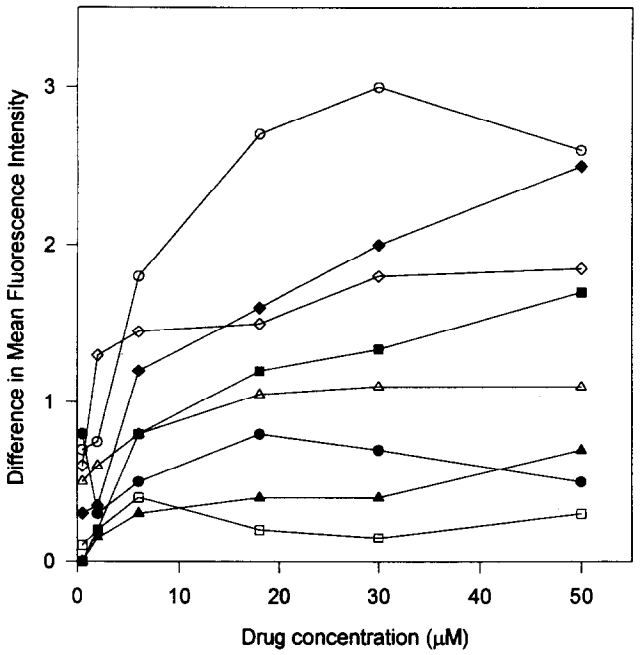


**FIG. 3. The ionophoretic activity of monensin and its derivatives was evaluated on living cells by cytofluorometry. The assay measured the ability of monensin or its derivatives to counteract the low pH-induced quenching of internalized Tfn-bound FITC. Results are expressed as difference in mean fluorescence intensity (ΔMFI) between untreated samples and samples treated with Tfn-FITC in the presence of monensin or its derivatives. Compounds are represented as those in Fig. 1.**

properties. This variability may be related principally to the structure of derivatives, but may also be influenced by the different intracellular routing of IT. Although no enhancers with greater activity than monensin are produced, these preliminary studies provide some guidance for the development of further monensin derivatives.

*This work was supported by MURST 40%–60%, by the Associazione Italiana per la Ricerca sul Cancro, and CNR grants (Progetti Finalizzati Biotecnologie e Biostrumentazione, Ingegneria Genetica, and A.C.R.O.).*

## References

1. Pietersz GA and McKenzie JFC, Antibody conjugates for the treatment of cancer. *Immunol Rev* **127:** 57–80, 1992.
2. Candiani C, Franceschi A, Chignola C, Pasti M, Anselmi C, Benoni G, Tridente G and Colombatti M, Blocking effect of human serum but not of cerebrospinal fluid on ricin A chain immunotoxin potentiation by monensin or carrier protein-monensin conjugates. *Cancer Res* **52:** 623–630, 1992.
3. Jansen FK, Blythman HE, Casellas P, Derocq JM and Dussossoy D, Enhancement of ITs: *in vitro* and *in vivo*. In: Membrane-mediated cytotoxicity (Eds. Bonavida B, Collier RJ), vol 45, pp. 167–173. Alan R. Liss Inc., New York, 1987.
4. Hara H and Seon BK, Complete suppression of *in vivo* growth of human leukemia cells by specific immunotoxin: nude mouse model. *Proc Natl Acad Sci USA* **84:** 3390–3394, 1987.
5. Griffin TW, Richardson C, Houston LL, LePage D, Bogden A and Raso V, Antitumor activity of intraperitoneal immunotoxin in a nude mouse model of human malignant mesothelioma. *Cancer Res* **47:** 4266–4270, 1987.
6. Griffin TW, Morgan AC and Blythman HE, Immunotoxin therapy assessment by animal models. In: *Immunotoxins* (Ed. Frankel AE), pp. 433–455. Kluwer Academic Publishers, Boston, 1988.
7. Hara H, Luo Y, Haruta Y and Seon BK, Efficient transplantation of human non-T leukemia cells into nude mice and induction of complete regression of the transplanted distinct tumors by ricin A chain conjugates of monoclonal antibody. *Cancer Res* **48:** 4673–4680, 1988.
8. Laurent G, Pris J, Farcet JP, Carayon P, Blythman H, Casellas P, Poncelet P and Jansen FK, Effects of therapy with T101-ricin A chain immunotoxin in two leukemic patients. *Blood* **67:** 1680–1687, 1986.
9. Spitler LE, Del Rio M, Khentigan A, Wedel NI, Brophy NA, Miller LL, Harkonen WS, Rosendorf LL, Lee HM, Mischak RP, Kawahata RT, Stoudemire JB, Fradkin LB, Bautista EE and Scannon PJ, Therapy of patients with malignant melanoma using a monoclonal antimelanoma antibody-ricin A chain immunotoxin. *Cancer Res* **47:** 1717–1723, 1987.
10. Weiner FM, O'Dwyer J, Kitson J, Comis RL, Frankel AE, Bauer RJ, Konrad MS and Groves ES, Phase I evaluation of an anti-breast carcinoma monoclonal antibody 260F9-recombinant ricin A chain immunoconjugate. *Cancer Res* **47:** 4062–4067, 1989.
11. Byers VS, Rodvien R, Grant K, Durrant LG, Hudson KH, Baldwin RW and Scannon PJ, Phase I study of monoclonal antibody-ricin A chain immunotoxin Xomazyme 791 in patients with metastatic colon cancer. *Cancer Res* **49:** 6153–6160, 1989.
12. Vitetta ES, Stone M, Amlot P, Fay J, May R, Till M, Newman J, Clark P, Collins R, Cunningham D, Ghetie V, Uhr JW and Thorpe PE, Phase I trial in patients with B cell lymphoma. *Cancer Res* **51:** 4052–4058, 1991.
13. LeMaistre CF, Rosen S, Frankel A, Kornfeld S, Saria E, Meneghetti C, Drajesk J, Fishwild D, Scannon P and Byers V, Phase I trial of H65-RTA immunoconjugate in patients with cutaneous T-cell lymphoma. *Blood* **78:** 1173–1182, 1991.
14. Ravel S, Colombatti M and Casellas P, Internalization and intracellular fate of anti-CD5 monoclonal antibody and anti-CD5-ricin A chain immunotoxin in human leukemic T cells. *Blood* **79:** 1511–1517, 1992.
15. Wargalla UC and Reisfeld RA, Rate of internalization of an immunotoxin correlates with cytotoxic activity against tumor cells. *Proc Natl Acad Sci USA* **86:** 5146–5150, 1989.
16. Ravel S and Casellas P, Internalization of cytotoxic molecules of T101-F(ab)'$_2$- (ricin A chain) immunotoxin into human T-leukemic cells. *Eur J Biochem* **192:** 469–473, 1990.
17. Press OW, Vitetta ES, Farr AG, Hansen JA and Martin PJ, Evaluation of ricin A-chain immunotoxin directed against human T cells. *Cell Immunol* **102:** 10–20, 1986.
18. Youle RJ and Neville DM, Role of endocytous and receptor recycling in ligand-toxin and antibody-toxin conjugate activity. In: *Immunoconjugates, Antibody conjugates in radioimaging and therapy of cancer* (Ed. Vogel C), pp. 153–169, Oxford University Press, New York, 1987.
19. Calafat J, Molthoff C, Janssen H and Hilkens J, Endocytosis and intracellular routing of an antibody-ricin A chain conjugate. *Cancer Res* **48:** 3822–3827, 1988.
20. Byers VS, Pawluczyk ZA, Hooi DSW, Price MR, Carrol S, Embleton MJ, Garnett MC, Berry N, Robin RA and Baldwin RW, Endocytosis of immunotoxin 79IT/36-RTA by tumor cells in relation to its cytotoxic action. *Cancer Res* **51:** 1990–1995, 1991.
21. Hwang KM, Foon KA, Cheung PH, Pearson JW and Olham RK, Selective antitumor effect on L10 hepatocarcinoma cells of a potent immunoconjugate composed of the A chain of abrin and a monoclonal antibody to a hepatoma-associated antigen. *Cancer Res* **44:** 4578–4586, 1984.

22. Pirker R, FitzGerald D, Hamilton T, Ozols R, Laird W, Frankel A, Willingham M and Pastan I, Characterization of immunotoxins active against ovarian cancer cell lines. *J Clin Invest* **76:** 1261–1267, 1985.
23. Henderson PJF, McGivan D and Chappel JB, Action of certain antibodies on mitochondrial, erythrocyte and artificial phospholipid membranes. Role of induced proton permeability. *Biochem J* **111:** 521–524, 1969.
24. Shavit N, Degani H and SanPietro A, Effects of ionophores antibiotics in chloroplasts. *Biochim Biophys Acta* **216:** 208–211, 1970.
25. Casellas P, Bourrie JP, Gros P and Jansen FK, Kinetics of cytotoxicity induced by immunotoxins. Enhancement by lysosomotropic amines and carboxylic ionophores. *J Biol Chem* **259:** 9359–9364, 1984.
26. Ramakrishnan S and Houston LL, Inhibition of human acute lymphoblastic leukemia cells by immunotoxin: potentiation by chloroquine. *Science* **223:** 58–61, 1984.
27. Colombatti M, Dell'Arciprete L, Chignola R and Tridente G, Carrier protein-monensin conjugates: enhancement of immunotoxin cytotoxicity and potential in tumor treatment. *Cancer Res* **50:** 1385–1391, 1990.
28. Mollenhauer HH, Morrè DJ and Rowe LD, Alteration of intracellular traffic by monensin: mechanism, specificity and relationship to toxicity. *Biochim Biophys Acta* **1031:** 225–246, 1990.
29. Jansen FK, Jansen A, Derocq JM, Carriere D, Carayon P, Veas F and Jaffrezou JP, Golgi vacuolization and immunotoxin enhancement by monensin and perhexilin depend on a serum protein. *J Biol Chem* **267:** 12577–12582, 1992.
30. Franceschi A, Dosio F, Anselmi C, Chignola R, Candiani C, Pasti M, Tridente G and Colombatti M, Mechanisms involved in serum-dependent inactivation of the immunotoxin enhances monensin and carrier-protein-monensin. *Eur J Biochem* **219:** 469–479, 1994.
31. Tartakoff AM, Perturbation of vesicular traffic with carboxylic ionophore monensin. *Cell* **32:** 1026–1028, 1983.
32. Brown MS, Anderson RGW and Goldstein JL, Recycling receptors: the round-trip itinerary of migrant membrane proteins. *Cell* **32:** 663–667, 1983.
33. Raso V and Lawrence J, Carboxylic ionophores enhance the cytotoxic potency of ligand and antibody-delivered ricin A chain. *J Exp Med* **160:** 1234–1240, 1984.
34. Tohda K, Suzuki K, Kosuge N, Watanabe K, Nagashima H, Inoue H and Shirai T, Design and synthesis of lithium ionophores for an ion-selective electrode by chemical modification of natural carboxylic polyether antibiotic monensin. *Anal Chem* **62:** 936–942, 1990.
35. Biagi GL, Guerra MC and Barbaro AM, Relationship between lipophilic character and hemolitic activity of testosterone esters. *J Med Chem* **13:** 944–948, 1970.
36. Biagi GL, Barbaro AM and Guerra MC, Partition data of cephalosporins determined by means of reversal-phase thin-layer chromatography. *J Chromat* **44:** 195–198, 1969.
37. Antin JH, Bierer BE, Smith BR, Guinan EC, Provost MM, Ferrara J, Macklis R, Tarbell NJ, Blythman H, Bouloux C, Zinniti LM, Bogart RE, Burakoff S and Weinstein H, Depletion of bone marrow T-lymphocytes with an anti CD5 antibody (ST-1 IT): effective prophylaxes for graft-versus-host disease. *Prog Clin Biol Res* **333:** 207–216, 1990.
38. Colombatti M, Bisconti M, Dell'Arciprete L, Gerosa M and Tridente G, Sensitivity of human glioma cells to cytotoxic heteroconjugates. *Int J Cancer* **42:** 441–448, 1988.
39. Klausner RD, van Renswoude J, Ashwell G, Kempf C, Schechter AN, Dean A and Bridges KR, Receptor-mediated endocytosis of transferrin in K562 cells. *J Biol Chem* **258:** 4715–4724, 1983.
40. Ohkuma S and Poole B, Fluorescence probe measurement of the intralysosomal pH in lung cells and the perturbation of pH by various agents. *Proc Natl Acad Sci USA* **73:** 3327–3331, 1978.
41. Chignola R, Colombatti M, Dell'Arciprete L, Candiani C and Tridente G, Distribution of endocytosed molecules to intracellular acidic environments correlates with immunotoxin activity. *Int J Cancer* **46:** 1117–1123, 1990.
42. Hertler AA, Frankel AE, Immunotoxins: a clinical review of their use in the treatment of malignancies. *J Clin Oncol* **7:** 1932–1935, 1989.
43. Uckun FM and Frankel AE, The current status of immunotoxins: an overview of experimental and clinical studies as presented at the Third International Symposium on immunotoxins. *Leukemia* **7:** 341–345, 1993.
44. Griffin TW, Childs LR, FitzGerald DJP and Levin LV, Enhancement of the cytotoxic effect of anti-carcinoembrionic antigen immunotoxin by adenovirus and carboxylic ionophores. *J Natl Cancer Inst* **79:** 679–685, 1987.
45. Carriere D, Casellas P, Richer G, Gros P, Jansen FK, Endocytosis of an antibody ricin A-chain conjugate (immuno-A-toxin) adsorbed on colloidal gold. Effects of ammonium chloride and monensin. *Exp Cell Res* **156:** 327–340, 1985.
46. Dautry-Varsat A, Ciechanover A, Lodish HF, pH and the recycling of transferrin during receptor-mediated endocytosis. *Proc Natl Acad Sci USA* **80:** 2250–2262, 1983.
47. Nakamura A, Nagai S, Takahashi T, Malhan R, Murakami N, Ueda T, Sakakibara J and Asano M, Studies on the chemical modification of monensin IV. Synthesis, sodium ion-permeability and biological activity of 7-O-acyl and 7-O-alkyl monensins. *Chem Pharm Bull* **40:** 2331–2337, 1992.
48. Sandvig K, Olsnes S and Pihl A, Inhibitory effect of ammonium chloride and chloroquine on the entry of the toxic lectin moddecin into HeLa cells. *Biochem Biophys Res Comm* **90:** 648–655, 1979.